

Learning to Cluster Faces via Transformer

Jinxing Ye^{*1}, Xiaojiang Peng^{*2}, Baigui Sun¹, Kai Wang^{1,3}, Xiuyu Sun¹, Hao Li ^{†1}, and Hanqing Wu¹

¹Alibaba Group

²Shenzhen Technology University, China

³National University of Singapore, Singapore

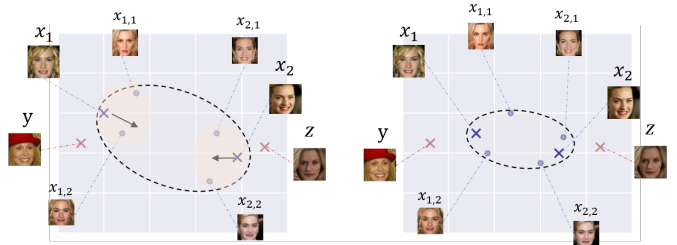
Abstract

*Face clustering is an useful tool for applications like automatic face annotation and retrieval. The main challenge is that it is difficult to cluster images from the same identity with different face poses, occlusions, and image quality. Traditional clustering methods usually ignore the relationship between individual images and their neighbors which may contain useful context information. In this paper, we repurpose the well-known Transformer and introduce a Face Transformer for supervised face clustering. In Face Transformer, we decompose the face clustering into two steps: relation encoding and linkage predicting. Specifically, given a face image, a **relation encoder** module aggregates local context information from its neighbors and a **linkage predictor** module judges whether a pair of images belong to the same cluster or not. In the local linkage graph view, Face Transformer can generate more robust node and edge representations compared to existing methods. Experiments on both MS-Celeb-1M and DeepFashion show that our method achieves state-of-the-art performance, e.g., 91.12% in pairwise F-score on MS-Celeb-1M.*

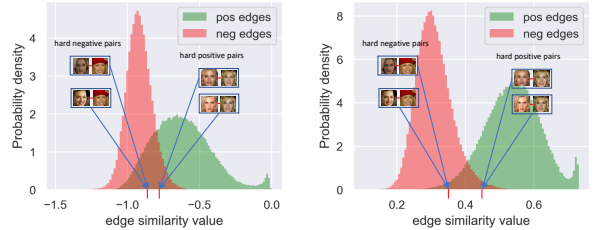
1. Introduction

In recent years, face recognition has achieved remarkable progress in real-world applications due to the development of advanced metric learning methods [7] and deep neural models [14]. Large-scale well-labelled data is very crucial for high-performance face recognition system, while to annotate these large-scale datasets is time-consuming and expensive. Recent solutions resort to clustering methods aiming to mine identity information from unlabeled data.

Traditional clustering methods generally make different assumptions on the input features. K-Means [19]



(a) Transfer features with context to cluster challenging samples.



(b) Adapt edge embedding via context to ease linkage prediction.

Figure 1. Illustration for implementing context-based node augmentation and edge augmentation in face clustering. (a) Face feature distribution in wild usually exists considerable challenging samples, which is hard to present direct clustering procedure. Transferring features with its local context is helpful to cluster those challenging samples. Images from the same ID are represented by the same letters. (b) Similarity between hard positive pairs and hard negative pairs usually gathered closely, which makes it difficult to decide a threshold to distinguish whether a link could be built. Adapting edge embedding via context eases linkage prediction task.

requires the distribution of clusters to be convex, DBSCAN (Density-Based Spatial Clustering of Applications with Noise) [8] requires the density within the cluster to be greater than a certain threshold, Spectral Clustering [24] requires clusters are of the similar sizes. However, in real-world applications, there still exist considerable images with extreme exposure, occlusion, pose variant, and

^{*}Equally-contributed first authors

[†]Corresponding author (lihao.lh@alibaba-inc.com)

low resolution, whose distributions are often too complex to meet these distribution assumptions. We call those hard samples as challenging samples. Clustering with these challenging samples may lead to the following problems[4]. First, challenging samples of the same person are inevitably far from the high-quality ones, resulting in splitting the same identity. Second, challenging images from different identities may be close to each other due to the dominant imaging condition, resulting in a degradation in purity. Third, the distance between an image and its neighbors differs from images to images, which leads to different merging threshold for different instances. The pioneer work Rank-Order [39] and recent supervised face clustering work [27] attempt to re-measure distance between samples via contextual information and annotations. However, they largely ignore that noise may exists in local neighbor topology, and directly consider all samples equally.

In this paper, considering contextual information is critical for clustering on a complex distribution, we re-purpose the well-known Transformer [26] and propose a uniform face clustering framework, termed as Face Transformer (FaceT). As shown in Figure 1, the key motivation of FaceT is to leverage contextual information contained in the local topology to reduce the adverse effects of challenging images thus to learn robust and compact cluster embeddings. To this end, FaceT contains two crucial modules: (i) Relation Encoder (RE) and (ii) Linkage Predictor (LP). Relation encoder is a transformer for a node to aggregate local context information from its neighbors. As illustrated in figure 1(a), RE increases the inter-class distance and reduce the intra-class distance between samples based on their context. Linkage predictor is a transformer for a node to judge whether a neighbor belongs to the same cluster or not. As illustrated in figure 1(b), LP improves the similarity between challenging samples and its positive samples and decreases the similarity with its negative samples.

Compared to these GCN-based supervised clustering models[27, 32, 31, 11] which need constructing adjacency matrices, our method is simpler and effectively inherits contextual information with the two transformer modules. We conduct extensive experiments with varied recognition models and training datasets, and achieve consistent improvements over related state-of-the-art methods on several widely-used benchmarks.

Our contributions can be summarized as follows:

- A node enhancement structure termed Relation Encoder(RE) is proposed, which extracts the contextual information of local topical structure to enhance node embedding.
- A Linkage Predictor(LP) that is composed of an edge enhancement structure and linkage classifier is proposed, which regards the clustering task as a linkage

prediction task and generalizes more precise predictions with enhanced edge embedding.

- A uniformed clustering framework, *i.e.* FaceT, achieves state-of-the-art performance with pairwise F-score 91.18, Bcubed F-score 90.54, NMI 97.63 on MS-Celeb-1M dataset.

2. Related Work

We first briefly review face clustering methods including unsupervised and supervised ones, and then present some related work on linkage prediction from social network analysis.

2.1. Face Clustering

Unsupervised methods. With the development of deep learning, recent works primarily adopt features extracted by a deep convolutional neural network (DCNN) [7, 22]. For the deep feature based clustering task, traditional algorithms like K-Means, spectral clustering, and DBSCAN usually lie on different data assumptions that are difficult to satisfy. Therefore, later methods usually focus on additional contextual information to cluster faces. Rank-order[39] proposed a relation metric approach based on the local context, ARO [20] proposed an approximate rank-order metric to reduce rank-order running cost, DDC [16] uses minimal covering spheres of neighborhoods as the similarity metric, PHAC [17] exploits neighborhood similarity based on linear SVMs that separates local positive instances and negative instances. Additional deep neural networks(DNNs) are recently used to boost clustering results, including unsupervised and supervised approaches. As typical unsupervised ones, DEC [29] and SDLC [30] use encoder-decoder structures to learn low-dimensional embeddings and cluster assignments. In general, there have been many schemes that adjust node representation based on context and have made some progress. However, those methods depend on hand-craft information communicating policy and usually treat each node equally, making it sensitive to outliers. Therefore, such methods usually have limited performance on face clustering tasks in wild.

Supervised methods. As recent supervised ones, some methods use contextual information to enhance the node embedding, so as to obtain a node representation that is more friendly to clustering. VE-GCN [31] uses two stacked GCNs to estimate vertices' confidence and build edges by those high-confidence vertices, DA-NET [11] uses stacked GCNs and LSTMs to decrease class intra-distance then generate better clustering results based on traditional algorithms. Other methods focus on the context-based distance metric method and try to obtain a more powerful distance measurement scheme. LGCN [27] proposed a linkage-based GCN to predict the linkage between a pivot node

and its neighbors via enhanced edge embeddings. Finally, some methods involve new clustering frameworks. After the clustering results are constructed using traditional methods, additional post-processing models are used to obtain more accurate clustering results. DS-GCN [32] is a typical work of this method, it learns to cluster in a detection-segmentation paradigm based on overlapped cluster proposals. Our method differs from the previous GCN-based approaches, FaceT doesn't suffer from constructing adjacency matrix and combines the advantages of the first two methods, which is more direct and effective.

2.2. Linkage Prediction

As a key problem in social network analysis, the objective of link prediction is to identify pairs of nodes that will either form a link or not. PageRank [21] and SimRank [15] analyze the whole graph via various information propagation approaches, preferential attachment [3] and resource allocation [38] analyze linkage probability only from local topical graph structure. Further work like Weisfeiler-Lehman Neural Machine [36] and LGNN [37] believe that it is sufficient to compute link likelihood only from the local neighborhood of a node pair and solve this task via various neural networks, GKC [34] calculate the graph kernel similarities between subgraphs and use an SVM to decide each linkage. In general, there have been a lot of linkage prediction related work proposed and verified in the field of social networks, but there are relatively few works related to face recognition and clustering.

3. Methodology

In large-scale face clustering, supervised approaches demonstrate their effectiveness with various mechanisms. Some supervised approaches[32] can handle complex patterns of clusters, but rely on manual components and large number of overlapping sub-graphs, which is time-consuming. Other light-GCN-based methods [27, 31, 11] can improve the speed of clustering, but are unable to consider both node and edge representations at the same time. To address the problem, we propose a simple yet efficient model: Face Transformer (FaceT). In FaceT, we divide the clustering task into two steps. First, we apply Relation Encoder (RE) to fuse contextual information for a node with original features from its neighbors. Then, Linkage Predictor (LP) is designed to determine whether paired nodes belong to the same ID or not.

3.1. Overview

FaceT aims to generate accurate paired linkage predictions using two well-designed modules. Given a dataset \mathcal{D} , we extract deep features of images by a pretrained DCNN model. Let $\mathcal{F} = \{f_i\}_{i=1}^N$ as feature set where $f_i \in \mathbb{R}^D$, D denotes the dimension of each image and N denotes the

number of images. For each sample feature f_q , we find its hop_1 nearest neighbor nodes by comparing their features similarities in \mathcal{F} , which are regarded as the candidate samples for final possible linkages. For query feature f_q and those hop_1 neighbors, we utilize the same manner to search the hop_2 nearest neighbor nodes for f_q and its candidate samples, respectively, which is a scalable schema. Then we replace query feature f_q with enhanced feature g_q generated by RE. For all hop_1 candidates, we apply the same manner and generate enhanced candidate features. As the enhanced query feature and its enhanced neighbors are generated, the LP is designed to assign linkage probabilities between query sample and its hop_1 candidate samples. Finally, the obtained probability is used as the similarity score to determine if the candidate is connected to this query pivot. Given a threshold τ , we form the link between query sample and a candidate sample whose pair linkage probability is larger than τ . By repeating the above process while treating all samples as query samples, we can get the linkage predictions on the entire test set. Finally, clustering procedure with linkage predictions could be done with Union-Find algorithm [9].

The key challenge for the proposed method remains in how to aggregate local context into node embeddings and edge embeddings. As shown in Figure 2, our framework consists of two learnable modules, namely Relation Encoder(RE) and Linkage Predictor(LP). The former module aggregates local context information from its neighbors, and the latter module judges whether a pair of images belong to the same cluster or not.

3.2. Transformer Preliminary

Assume we have n query vectors each with dimension $d_q : Q \in \mathbb{R}^{n \times d_q}$, we can define an attention function $\mathcal{A}(Q, K, V)$ to calculate similarity between instance pairs.

$$\mathcal{A}(Q, K, V; \omega) = \omega(QK^\top)V \quad (1)$$

There $K \in \mathbb{R}^{n_v \times d_1}$, $V \in \mathbb{R}^{n_v \times d_v}$ are n_v key-value pairs, ω is an activation function, the output $\omega(QK^\top)V$ is a weighted sum of value vectors, where an instance value would get more weight when its key has larger dot product with the query vector. For multi-head attention $\mathcal{M}(\cdot, \cdot, \cdot; \lambda)$, first project Q, K, V onto h different d_q^M, d_k^M, d_v^M -dimensional vectors, then apply an attention function $\mathcal{A}(\cdot; \omega_j)$ to each of these h projections, finally reduce dimension with a linear transformation as follows:

$$\mathcal{M}(Q, K, V; \lambda, \omega) = \text{cat}(O_1, \dots, O_h)W^O \quad (2)$$

where,

$$O_i = \mathcal{A}(QW_i^Q, KW_i^K, VW_i^V; \omega_i) \quad (3)$$

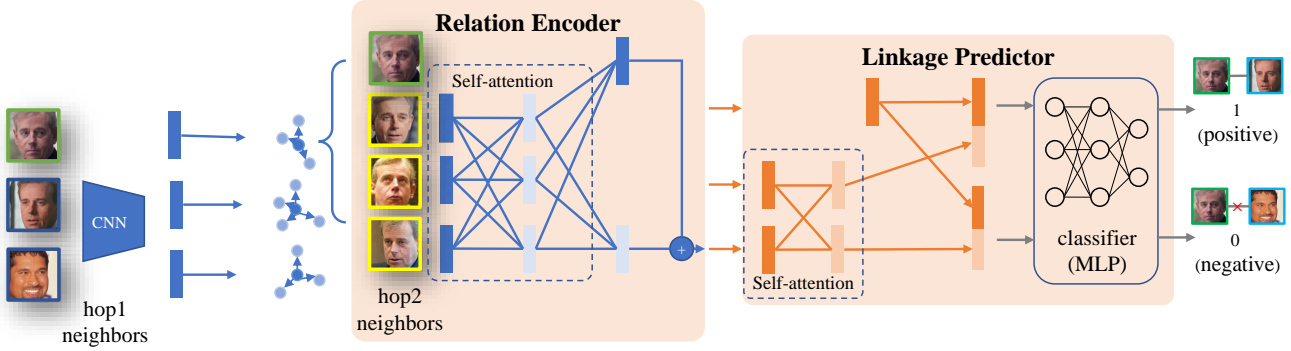


Figure 2. The overview of Face Transformer architecture. For each original face feature f_q , we first enhance it with its local context (constructed by $hop2$ nearest neighbors) resulting in enhanced feature g_q . Then for each node f_q , we use its $hop1$ neighbors as linkable candidates, then calculate linkage likelihood with their respective enhanced features via Linkage Predictor. Finally, we use the linkage likelihood to generate output clusters with the Union-Find algorithm. (In this toy example, $hop1$ is 2 and $hop2$ is 3.)

There $cat(\cdot, \cdot)$ represents concatenation operation along the feature dimension. Note that $\mathcal{M}(\cdot, \cdot, \cdot; \lambda)$ has learnable parameters $\lambda = \{W_i^Q, W_i^K, W_i^V\}_{i=1}^h$, where $W_i^Q, W_i^K \in \mathbb{R}^{d_q * d_q^M}$, $W_i^V \in \mathbb{R}^{d_v * d_v^M}$, $W^O \in \mathbb{R}^{hd_v^M * d}$. Unless otherwise specified, we use a scaled softmax $\omega_i(\cdot) = softmax(\frac{\cdot}{\sqrt{d}})$.

3.3. Relation Encoder

Relation Encoder(RE) is used for enhancing node representations, which consists of d_e self-attention layers and one normal attention layer. Its structure is illustrated in figure 3(a). For each node embedding f_q to be enhanced, first we find its $hop2$ neighbors $f_{q,1}, f_{q,2}, \dots, f_{q,hop2}$ from \mathcal{F} with normal retrieval methods. Then, we use self-attention layers to enhance $f_{q,j}$, where $j \in \{1, 2, \dots, hop2\}$.

Apart from the attention functions mentioned in 3.2, we apply dropout to each sub-layers output before it is added to the sub-layer input and normalized. We employ a residual connection around each of the two sub-layers, followed by layer normalization. In following method, dropout function is represented as $d(\cdot)$, layer normalization function is represented as $\mathcal{N}_L(\cdot)$. First, we use self-attention layers to enhance original face features, which can be formulated as:

$$f_{q,k}^l = \mathcal{N}_L(d(\mathcal{M}(f_{q,k}^{l-1}, K^{l-1}, V^{l-1})) + f_{q,k}^{l-1}) \quad (4)$$

There $f_{q,k}^l$ denotes self-attention layer output from the $l - th$ layer, $l \in \{1, 2, \dots, d_e\}$, $f_{q,k}^0 = f_{q,k}$, K, V denotes all $hop2$ neighbors' key vectors and value vectors. Next, we will use a common attention layer to construct the query's context representation, denotes as \tilde{f}_q . Finally, we use an add and norm operation to generate enhanced face feature g_q , formulated as:

$$\tilde{f}_q = (\mathcal{M}(f_q, K^{d_e}, V^{d_e})) \quad (5)$$

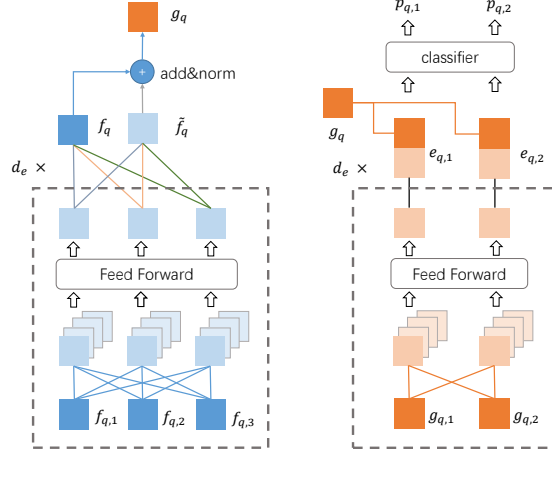


Figure 3. Details of Relation Encoder and Linkage Predictor.

$$g_q = \mathcal{N}(\tilde{f}_q + f_q) \quad (6)$$

3.4. Linkage Predictor

Linkage Predictor(LP) is used for enhancing edge representations and predicting linkages, which consists of d_e self-attention layers and one MLP working as a linkage classifier. Its structure is illustrated in figure 3(b). This module is applied to decide whether a neighbors' enhanced face feature $g_{q,k}$ could build a connection with the enhanced query face feature g_q . First, we find $hop1$ nearest neighbors of query feature f_q from \mathcal{F} and replace them with related enhanced face features generated by RE. Secondly, self-attention layers are applied to enhanced neighbors' features, get g_k^l , formulated as:

$$g_{q,k}^l = \mathcal{N}_L(d(\mathcal{M}(g_{q,k}^{l-1}, K, V)) + g_{q,k}^{l-1}) \quad (7)$$

There $g_{q,k}^l$ denotes self-attention layer output from the $l-th$ layer, $l \in \{1, 2, \dots, d_e\}$, specially, $g_{q,k}^0 = g_{q,k}$, K, V denotes all *hop1* neighbors' key vectors and value vectors. Then, concatenate g_q and $g_{q,k}^l$ to generate edge embedding $e_{q,k}$, defined as:

$$e_{q,k} = \text{cat}(g_k, g_{q,k}^{e_d}) \quad (8)$$

Finally, use a 2-layer MLP to predict probability $p_{q,k}$ of the $e_{q,k}$, which is formulated as:

$$p_{q,k} = \omega(\mathcal{C}(e_{q,k})) \quad (9)$$

There $\mathcal{C}(\cdot)$ is a two-layer MLP using an edge embedding $e_{q,k}$ as input, output probability $p_{q,k}$ of the input edge is positive. We use PReLU [13] as activation function in our method.

3.5. Complexity Analysis

For both RE and LP, we need to construct a KNN graph; this needs to be done only once. Hence, its complexity can be regarded as $O(n \log n)$ by Approximate Nearest Neighbor (ANN) search. Like the previous work LGCN, the proposed method is only processed on the local topical subgraph. Hence the runtime of the link prediction process grows linearly with the number of data. Therefore, the total complexity of our pipeline is $O(n \log n)$ considering ANN cost, $O(n)$ for ignoring ANN cost, n marks instance amount of \mathcal{D} .

4. Experiments

4.1. Experimental Settings

Face Clustering. MS-Celeb-1M [12] is a large-scale face recognition dataset consisting of 100K identities and 5.8M images. As previous work DS-GCN and VE-GCN did, we adopt the widely used annotations from ArcFace [7] that contains 5.8M images from 86K classes. The cleaned dataset was randomly split into ten parts, with an almost equal number of identities. To make a fair comparison, we use the same data released by DS-GCN and VE-GCN ¹, details of those datasets are listed in Table 1, subset 0 is adopted for training face recognition model and clustering model, the others is used for testing. We use ArcFace[7] as the face representations with dimension of 256.

Besides, we tested our method with additional DCNN model to validate the scalability of our method. We use ArcFace[7] as the face representations with dimension of

Table 1. Details of MS-Celeb-1M subsets.

id	0	1	3	5	7	9
#id	8.6K	8.6K	25.7K	42.9K	60.0K	77.2K
#inst	576K	584K	1.74M	2.89M	4.05M	5.21M

512. This model is trained on the union set of MS-Celeb-1M [12] and VGGFace2[5] dataset. For a fair comparison, we use the data provided by LGCN[27] ². Our FaceT is trained on CASIA dataset[33] and tested on IJB-B dataset[28]. IJB-B consists of three sets, which include 512, 1,024, 1,845 identities, and 18,171, 36,575, 68,195 samples. We follow its official protocol[28] for evaluation.

Fashion Clustering. We also evaluate the effectiveness of our method over the non-face dataset. We adopted the large subset of DeepFashion [18], a long-tail clothes retrieval dataset. To make a fair comparison, we use the same data released by DS-GCN and VE-GCN ¹. Training features and testing features are mixed in the original split and randomly sample 25, 752 images from 3, 997 categories for training, and the other 26, 960 images with 3, 984 categories for testing. Because fashion clustering is regarded as an open set problem, there is no overlap between training categories and testing categories.

Evaluation Metrics. To evaluate the performance of the proposed clustering algorithm, we adopt three mainstream evaluation metrics: BCubed Fmeasure [1], pairwise Fmeasure [2] and normalized mutual information(NMI).

NMI is a widely used metric that measures the normalized similarity two sets, given Ω the ground truth cluster set, C the prediction cluster set, $H(\Omega)$ and $H(C)$ are their entropies, $I(\Omega, C)$ represents the mutual information. NMI is calculated as follows.

$$NMI(\Omega, C) = \frac{I(\Omega, C)}{\sqrt{H(\Omega)H(C)}} \quad (10)$$

We did not evaluate traditional methods with the NMI measure metric on the MS1M benchmark. For the IJB-B benchmark, $F_{512}, F_{1024}, F_{1845}$ are Bcubed F-scores of different sets.

Implementation Details. To train the FaceT, we set the depth of encoders d_e as 2, both for RE and LP. Our feature dimension is 256, attention head dimension is 64, attention head amount is 4, and the dropout ratio is 0.4. For IJB-B experiments, our feature dimension is 512, attention head dimension is 128, the other hyper parameter settings remain the same.

We adopt a linear learning rate warm-up for the first 500 steps for the training phase, then use cosine decay policy for the rest training epochs. The batch size is 32; the weight decay parameter is 0.0005. For MS-Celeb-1M and CASIA

¹<https://github.com/yli-1993/learn-to-cluster>

²https://github.com/Zhongdao/gcn_clustering

dataset, we adopt $hop1 = 150$, $hop2 = 5$, training for 60 epochs with a base learning rate 0.002; for DeepFashion dataset, we use $hop1 = 8$, $hop2 = 6$, training for 1200 epochs with a base learning rate 0.02.

4.2. Method Comparison

Like the previous works, we compare our method with several baseline methods, each with a brief description. For all those methods, we tune the hyper-parameters and report the best results.

K-Means [19] is a commonly used clustering algorithm. For $N \geq 1.74M$, we use mini-batch K-means [23], which can reduce running time by running the original K-Means algorithm with mini-batches.

HAC [25] hierarchically merges close clusters based on various criteria in a bottom-up manner.

DBSCAN [8] recognize clusters from the gallery based on a designed density criterion, then leave the isolated point.

MeanShift [6] updates candidates for centroids to be the mean of the points within a given region.

AP [10] creates clusters by sending messages between pairs of samples until convergence.

Spectral Clustering [24] performs a low-dimension embedding of the affinity matrix between samples, followed by clustering of the components of the eigenvectors in the low dimensional space.

DDC [16] performs clustering based on measuring density affinities between local neighborhoods in the feature space.

ARO [20] performs clustering with an approximate nearest neighbor search and a modified distance measure.

CDP [35] performs clustering by exploiting a more robust pairwise relationship via gathering different predictions.

LGCN [27] is a supervised clustering method that adopts GCNs to exploit graph context for pairwise prediction, then performs clustering based on the output pairwise prediction.

DS-GCN [32] is a supervised clustering method that formulates clustering as a detection and segmentation pipeline.

VE-GCN [31] proposes a method that employs a stacked GCN architecture to estimate the connectivity and obtain clusters by connecting each node to the most connective neighbors in the candidate set.

FaceT is the proposed method that uses a hierarchical transformer architecture to enhance node embedding and edge embedding synchronously and build connections on enhanced pairwise linkage predictions.

4.3. Results

For all methods, we tune the corresponding hyper-parameters and report the best results. The results in Table 2, Table 3, and Table 4 show: (1) As is conducted in [32, 31], traditional methods including K-Means, DBSCAN, Spectral and ARO are limited in number of clusters assumptions, distribution assumptions or large com-

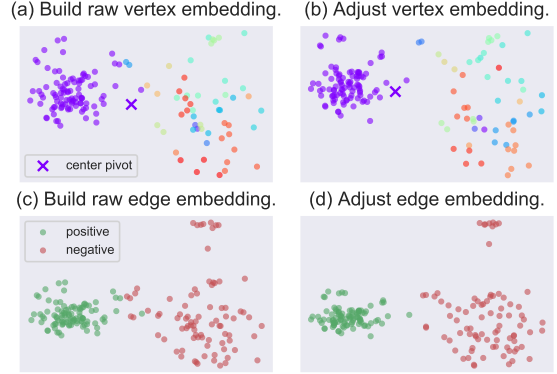


Figure 4. Adjust node and edge embedding with our method. (a) Original features as node embeddings, where samples from the same category are marked in the same color. (b) Enhanced node feature embeddings generated by RE. (c) Raw edge embeddings by concatenating paired node features. (d) Enhanced edge feature embeddings generated by LP. Our method makes node of the same class concentrate more tightly; meanwhile, the positive and negative edge embedding interface is more explicit. This affinity graph is built on a random center pivot’s local topical subgraph of MS1M dataset subset 1.

putational budget, which make them hard to use in real-world situations. (2) CDP is quite efficient and achieves considerable F-scores on different datasets. (3) L-GCN and DS-GCN surpasses CDP consistently but they are an order of magnitude slower than CDP. (4) VE-GCN yields superior performance, and has a high operating efficiency benefit from its high-confidence sample screening strategy. (5) The proposed FaceT outperforms previous methods consistently. Although the training set of FaceT only contains 584K images 2, it scales well to 5.21M unlabeled data, demonstrating its effectiveness in capturing contextual information of nodes and edges and predicting linkages.

For results on IJB-B in Table 4, L-GCN[27] uses the down-sampled CASIA training set, while sampling details is not provided, we randomly make three down-sampled subsets for training and take the best result to report. Therefore, comparison on IJB-B benchmark is not fair enough to make a solid conclusion due to the unaligned down-sampling policy, and we should focus on datasets that can be fairly compared, such as MS1M 2. What’s more, DANET[11] used completely different feature and training set, therefore it is hard to make a fair comparison between DANET and the other methods.

4.4. Ablation Study

In order to verify that key modules work as expected and study some key design choices, we conduct ablation study on MS-Celeb-1M subset 1. The ablation experiments is conducted from two aspects, the validity of the model structure and the influence of model hyper-parameters.

Table 2. Comparison on MS-Celeb-1M with different numbers of unlabeled images, subset id remarks different sizes. 1,3,5,7,9 respectively represent images count of 584K, 1.74M, 2.89M, 4.05M and 5.21M .

Method	pairwise F-score(F_P)					BCubed F-score(F_B)					NMI					Time
	1	3	5	7	9	1	3	5	7	9	1	3	5	7	9	
K-Means	79.21	73.04	69.83	67.9	66.47	81.23	75.2	72.34	70.57	69.42	-	-	-	-	-	11.5h
HAC	70.63	54.4	11.08	1.4	0.37	70.46	69.53	68.62	67.69	66.96	-	-	-	-	-	12.7h
DBSCAN	67.93	63.41	52.5	45.24	44.94	67.17	66.53	66.26	44.87	44.74	-	-	-	-	-	1.9m
ARO	13.6	8.78	7.3	6.86	6.35	17	12.42	10.96	10.5	10.01	-	-	-	-	-	27.5m
CDP	75.02	70.75	69.51	68.62	68.06	78.70	75.82	74.58	73.62	72.92	94.69	94.62	94.63	94.62	94.61	2.3m
L-GCN	78.68	75.83	74.29	73.70	72.99	84.37	81.61	80.11	79.33	78.60	96.12	95.78	95.63	95.57	95.49	63.8m
DS-GCN	87.61	83.76	81.62	80.33	79.21	87.76	83.99	82.00	80.72	79.71	97.04	96.55	96.33	96.18	96.07	47.3m
VE-GCN	87.93	84.04	82.1	80.45	79.30	86.09	82.84	81.24	80.09	79.25	96.41	96.03	95.85	95.71	95.62	11.5m
FaceT	91.12	89.07	86.78	84.10	83.86	90.50	86.84	85.09	84.67	83.86	97.61	97.12	96.87	96.82	96.67	28.0m

Table 3. Comparison on IJB-B.

Method	F_{512}	F_{1024}	F_{1845}
K-means	61.2	60.3	60.0
DBSCAN	75.3	72.5	69.5
Spectral	51.7	50.8	51.6
AP	49.4	48.4	47.7
ARO	76.3	75.8	75.5
DDC	80.2	80.5	80.0
LGCN	83.3	83.3	81.4
FaceT	83.1	83.3	82.2

Table 4. Comparison on DeepFashion.

Method	F_P	F_B	NMI
K-means	32.02	53.30	88.91
HAC	22.54	48.77	90.44
DBSCAN	25.07	53.23	90.75
MeanShift	31.61	56.73	89.29
Spectral	29.60	47.12	86.95
ARO	25.04	52.77	88.71
CDP	28.28	57.83	90.93
LGCN	30.7	60.13	90.67
DS-GCN	33.25	56.83	89.36
VE-GCN	38.47	60.06	90.50
FaceT	34.82	61.29	91.28

Visual Analysis. Regarding the impact of our method, we give a visual analysis in Figure 4. We randomly selected the center point of a batch and its neighbors of hop1, and visualized the point embedding and edge embedding. As is shown in Figure 4, after adjustment by Face Transformer, the sample variance of the same category as the center point becomes smaller, and the boundary between positive and negative samples on the edge embedding interface becomes clearer, which means those ambiguous samples are easier to be separated after those two adjustments.

Relation Encoder and Linkage Predictor. To better evaluate each sub structure’s role, we conduct end-to-end experiments using each sub-module separately. Because our method is composed of RE and LP structures in series,

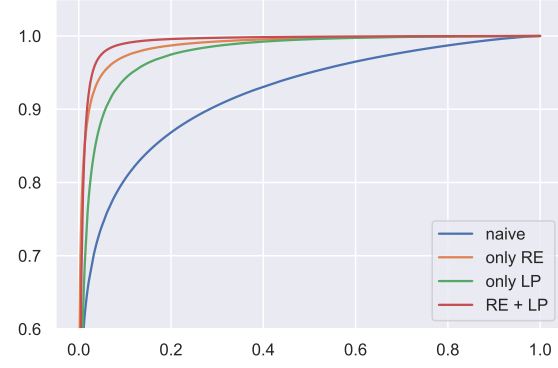


Figure 5. ROC of Linkage prediction on MS-Celeb-1M.

Table 5. Compatibility analysis on MS-Celeb-1M.

Method	F_P	F_B	NMI
naive	70.63	70.46	92.67
only RE	86.17	87.29	96.72
only LP	82.08	80.72	94.72
RE+LP	91.12	90.50	97.61

using these two sub-modules independently requires separate retraining. For validating the effectiveness of LP, we trained a model with only one Relation Encoder structure, which is termed as **only RE**. For validating the effectiveness of RE, we trained a model with only one Linkage Predictor structure, which is termed as **only LP**. Training policy and hyper-parameters are the same as the original FaceT. An end-to-end clustering test is shown in Table 5.

In order to properly train **only RE** model, we need to introduce a new training objective function to complete end-to-end training. We first normalize of node features with L2 normalize function \mathcal{N} , then use the L2 distance as the distance metric between the two nodes, finally convert this distance metric into a two-class probability distribution to use the same training strategy as the MLP-based two-classifier. The specific method could be described as follows.

$$e_{q,k} = 0.25 * \|\mathcal{N}(g_k) - \mathcal{N}(g_{q,k})\|_2^2 \quad (11)$$

$$p_{q,k} = (1 - e_{q,k}, e_{q,k}) \quad (12)$$

In the end-to-end test scenario, the complete FaceT architecture has obvious performance advantages. In the case of limited computing resources, using RE or LP alone can also achieve a particular effect. Additionally, we utilize the ROC curve to illustrate the discriminative power of our final linkage prediction approach. There, we use the top 80 predictions of each node on MS-Celeb-1M subset 1. As shown in Figure 5, under the same false-positive rate, the full FaceT architecture's true-positive rate is much higher than the other candidates.

Time Complexity Analysis. We measure the runtime of different methods with ES-2640 v3 CPU and Tesla V100 (16G). For MS1M, we measure the clock timings when N = 584K. (i.e. subset 1) Note that the clustering framework we used is similar to LGCN, which is based on the clustering task completed by linkage prediction and clustering post-processing, and it is quite different from DS-GCN and VE-GCN in clustering framework. The existing clustering methods have large differences in specific implementation and resource utilization, so it is not completely fair to directly compare the running time. Because our CPU environment is consistent, we directly use the speed measurement results of some methods in [31].

Hyper-parameters. To better understand our hyper-parameters, we set a group of parameters as our default setting, then alter one parameter while the others are fixed. We mainly study the influence of encoder depth (d_e), attention head amount(n_h), attention head dimension(d_h), dropout ratio(dr), training hop1($hop1$) and training hop2($hop2$). For the default method, ($d_e, n_h, d_h, \text{dropout}, hop1, hop2$) is set as (2, 4, 64, 0.4, 150, 5).

Table 6. Hyper parameter analysis. We alter only one hyper parameter to classify its robustness each time, F_P , F_B , NMI are different measure metrics.

	value	F_P	F_B	NMI
default	-	91.12	90.50	97.61
d_e	1	91.08	90.46	97.56
	4	91.07	90.39	97.57
n_h	2	91.12	90.37	97.47
	8	91.34	90.6	97.63
d_h	32	90.96	90.18	97.18
	128	91.07	90.6	97.63
dr	0.2	91.64	90.75	97.67
	0.6	89.96	89.96	97.47
$hop1$	120	91.18	90.39	97.58
	180	91.51	90.54	97.63
$hop2$	10	90.76	90.26	97.56
	20	89.03	89.23	97.29

From the listed experimental results in Table 6, our method is not sensitive to the encoder depth d_e . From our experimental results, reducing the numbers of self-attention layers in RE and LP will have a certain impact on the end-to-end test results. We believe that the self-attention layers can make the neighborhood topology between nodes smoother, thereby making the normal attention layer of RE and the MLP classifier of LP generate more accurate results. However, under the condition that other parameters are fixed, deepening the encoders will not bring substantial benefits. We believe that when d_e is set to 2, the model's fitting ability is already sufficient to learn the context distribution.

For the attention head related parameters, such as n_h and d_h , increasing the parameter scale can bring certain degree of performance improvement. It is a typical strategy of increasing the amount of calculation in exchange for performance improvement. However, it is observed that this improvement is not prominent, and trade-off should be decided on specific actual application scenarios.

For training hyper-parameter dr , we found that 0.4 used in the default settings may be too large. Broad regularization terms may limit the neural network model's learning ability, which may lead to under-fitting. From the listed experimental results, reducing the dropout ratio can slightly improve the performance on the test set.

For the heuristic parameters $hop1$ and $hop2$, the selected strategy is closely related to the data set. For $hop1$ neighbors, we expect the positive and negative samples to be balanced as much as possible while trying to make the model thoroughly learn some knowledge of difficult samples (i.e., positive samples with low similarity and negative samples with high similarity). During the training process, we found that loss tends to converge to a lower solution when $hop1$ is set to a small value, but it is difficult to thoroughly learn the knowledge of difficult samples, which leads to worse performance on the test set. For the nearest neighbors of $hop2$, we want them to come from the same category as the center point as much as possible, so this value is often set to a small value. Similar to the $hop1$ hyperparameter, during the training process, we found that increasing this hyper-parameter leads to a smaller loss converge, but performs worse on the test set. We think this phenomenon is caused by overfitting. When the number of neighbor samples used for training RE increases, a trivial solution may be learned from training samples that not from the same category of center pivot, limiting the performance of the model on the test set.

5. Conclusion and Future Work

In this work, we refer to the idea of Transformer applied in document classification and model the clustering task as a linkage prediction task. This paper proposes a novel method

to enhance the node and the edge representation simultaneously and achieve the most advanced performance on the face clustering task. Experiments on clustering scenarios have verified the effectiveness of the method. Besides, we notice that using RE alone obtains robust node representations that are measurable in Euclidean space. As iterative updating policy of KNN may obtain more accurate results, the specific algorithm framework is worthy of further exploration. Finally, there is still room for further improvement in the current method of hyper-parameter exploration. We will make further theoretical analysis and experimental exploration in the model structure design and hyper-parameter settings.

References

- [1] Enrique Amigó, Julio Gonzalo, Javier Artiles, and Felisa Verdejo. A comparison of extrinsic clustering evaluation metrics based on formal constraints. *Information retrieval*, 12(4):461–486, 2009. [5](#)
- [2] Arindam Banerjee, Chase Krumpelman, Joydeep Ghosh, Sugato Basu, and Raymond J Mooney. Model-based overlapping clustering. In *Proceedings of the eleventh ACM SIGKDD international conference on Knowledge discovery in data mining*, pages 532–537, 2005. [5](#)
- [3] Albert-László Barabási and Réka Albert. Emergence of scaling in random networks. *science*, 286(5439):509–512, 1999. [3](#)
- [4] Shai Ben-David and Nika Haghtalab. Clustering in the presence of background noise. In *International Conference on Machine Learning*, pages 280–288, 2014. [2](#)
- [5] Qiong Cao, Li Shen, Weidi Xie, Omkar M Parkhi, and Andrew Zisserman. Vggface2: A dataset for recognising faces across pose and age. In *2018 13th IEEE international conference on automatic face and gesture recognition (FG 2018)*, pages 67–74. IEEE, 2018. [5](#)
- [6] Yizong Cheng. Mean shift, mode seeking, and clustering. *IEEE transactions on pattern analysis and machine intelligence*, 17(8):790–799, 1995. [6](#)
- [7] Jiankang Deng, Jia Guo, Niannan Xue, and Stefanos Zafeiriou. Arcface: Additive angular margin loss for deep face recognition. In *Proceedings of the IEEE Conference on Computer Vision and Pattern Recognition*, pages 4690–4699, 2019. [1, 2, 5](#)
- [8] Martin Ester, Hans-Peter Kriegel, Jörg Sander, Xiaowei Xu, et al. A density-based algorithm for discovering clusters in large spatial databases with noise. In *Kdd*, volume 96, pages 226–231, 1996. [1, 6](#)
- [9] Michael Fredman and Michael Saks. The cell probe complexity of dynamic data structures. In *Proceedings of the twenty-first annual ACM symposium on Theory of computing*, pages 345–354, 1989. [3](#)
- [10] Frey, Brendan, J., Dueck, and Detbert. Clustering by passing messages between data points. *Science*, 2007. [6](#)
- [11] Senhui Guo, Jing Xu, Dapeng Chen, Chao Zhang, Xiaogang Wang, and Rui Zhao. Density-aware feature embedding for face clustering. In *Proceedings of the IEEE/CVF Conference on Computer Vision and Pattern Recognition*, pages 6698–6706, 2020. [2, 3, 6](#)
- [12] Yandong Guo, Lei Zhang, Yuxiao Hu, Xiaodong He, and Jianfeng Gao. Ms-celeb-1m: A dataset and benchmark for large-scale face recognition. In *European conference on computer vision*, pages 87–102. Springer, 2016. [5](#)
- [13] Kaiming He, Xiangyu Zhang, Shaoqing Ren, and Jian Sun. Delving deep into rectifiers: Surpassing human-level performance on imagenet classification. In *Proceedings of the IEEE international conference on computer vision*, pages 1026–1034, 2015. [5](#)
- [14] Kaiming He, Xiangyu Zhang, Shaoqing Ren, and Jian Sun. Deep residual learning for image recognition. In *Proceedings of the IEEE conference on computer vision and pattern recognition*, pages 770–778, 2016. [1](#)
- [15] Glen Jeh and Jennifer Widom. Simrank: a measure of structural-context similarity. In *Proceedings of the eighth ACM SIGKDD international conference on Knowledge discovery and data mining*, pages 538–543, 2002. [3](#)
- [16] Wei-An Lin, Jun-Cheng Chen, Carlos D Castillo, and Rama Chellappa. Deep density clustering of unconstrained faces. In *Proceedings of the IEEE Conference on Computer Vision and Pattern Recognition*, pages 8128–8137, 2018. [2, 6](#)
- [17] Wei-An Lin, Jun-Cheng Chen, and Rama Chellappa. A proximity-aware hierarchical clustering of faces. In *2017 12th IEEE International Conference on Automatic Face & Gesture Recognition (FG 2017)*, pages 294–301. IEEE, 2017. [2](#)
- [18] Ziwei Liu, Ping Luo, Shi Qiu, Xiaogang Wang, and Xiaoou Tang. Deepfashion: Powering robust clothes recognition and retrieval with rich annotations. In *Proceedings of the IEEE conference on computer vision and pattern recognition*, pages 1096–1104, 2016. [5](#)
- [19] Stuart Lloyd. Least squares quantization in pcm. *IEEE transactions on information theory*, 28(2):129–137, 1982. [1, 6](#)
- [20] Charles Otto, Dayong Wang, and Anil K Jain. Clustering millions of faces by identity. *IEEE transactions on pattern analysis and machine intelligence*, 40(2):289–303, 2017. [2, 6](#)
- [21] Lawrence Page, Sergey Brin, Rajeev Motwani, and Terry Winograd. The pagerank citation ranking: Bringing order to the web. Technical report, Stanford InfoLab, 1999. [3](#)
- [22] Florian Schroff, Dmitry Kalenichenko, and James Philbin. Facenet: A unified embedding for face recognition and clustering. In *Proceedings of the IEEE conference on computer vision and pattern recognition*, pages 815–823, 2015. [2](#)
- [23] David Sculley. Web-scale k-means clustering. In *Proceedings of the 19th international conference on World wide web*, pages 1177–1178, 2010. [6](#)
- [24] Jianbo Shi and Jitendra Malik. Normalized cuts and image segmentation. *IEEE Transactions on pattern analysis and machine intelligence*, 22(8):888–905, 2000. [1, 6](#)
- [25] Sibson and R. Slink: An optimally efficient algorithm for the single-link cluster method. *Comput. J.*, 16(1):30–34, 1973. [6](#)
- [26] Ashish Vaswani, Noam Shazeer, Niki Parmar, Jakob Uszkoreit, Llion Jones, Aidan N Gomez, Łukasz Kaiser, and Illia Polosukhin. Attention is all you need. In *Advances in neural information processing systems*, pages 5998–6008, 2017. [2](#)

- [27] Zhongdao Wang, Liang Zheng, Yali Li, and Shengjin Wang. Linkage based face clustering via graph convolution network. In *Proceedings of the IEEE Conference on Computer Vision and Pattern Recognition*, pages 1117–1125, 2019. [2](#), [3](#), [5](#), [6](#)
- [28] Cameron Whitelam, Emma Taborsky, Austin Blanton, Brianna Maze, and Patrick Grother. Iarpa janus benchmark-b face dataset. In *2017 IEEE Conference on Computer Vision and Pattern Recognition Workshops (CVPRW)*, 2017. [5](#)
- [29] Junyuan Xie, Ross Girshick, and Ali Farhadi. Unsupervised deep embedding for clustering analysis. In *International conference on machine learning*, pages 478–487, 2016. [2](#)
- [30] Bo Yang, Xiao Fu, Nicholas D Sidiropoulos, and Mingyi Hong. Towards k-means-friendly spaces: Simultaneous deep learning and clustering. In *international conference on machine learning*, pages 3861–3870. PMLR, 2017. [2](#)
- [31] Lei Yang, Dapeng Chen, Xiaohang Zhan, Rui Zhao, Chen Change Loy, and Dahua Lin. Learning to cluster faces via confidence and connectivity estimation. In *Proceedings of the IEEE/CVF Conference on Computer Vision and Pattern Recognition*, pages 13369–13378, 2020. [2](#), [3](#), [6](#), [8](#)
- [32] Lei Yang, Xiaohang Zhan, Dapeng Chen, Junjie Yan, Chen Change Loy, and Dahua Lin. Learning to cluster faces on an affinity graph. In *Proceedings of the IEEE Conference on Computer Vision and Pattern Recognition*, pages 2298–2306, 2019. [2](#), [3](#), [6](#)
- [33] Dong Yi, Zhen Lei, Shengcrai Liao, and Stan Z. Li. Learning face representation from scratch. *Computer ence*, 2014. [5](#)
- [34] Weiwei Yuan, Kangya He, Donghai Guan, Li Zhou, and Chenliang Li. Graph kernel based link prediction for signed social networks. *Information Fusion*, 46:1–10, 2019. [3](#)
- [35] Xiaohang Zhan, Ziwei Liu, Junjie Yan, Dahua Lin, and Chen Change Loy. Consensus-driven propagation in massive unlabeled data for face recognition. In *Proceedings of the European Conference on Computer Vision (ECCV)*, pages 568–583, 2018. [6](#)
- [36] Muhan Zhang and Yixin Chen. Weisfeiler-lehman neural machine for link prediction. In *Proceedings of the 23rd ACM SIGKDD International Conference on Knowledge Discovery and Data Mining*, pages 575–583, 2017. [3](#)
- [37] Muhan Zhang and Yixin Chen. Link prediction based on graph neural networks. In *Advances in Neural Information Processing Systems*, pages 5165–5175, 2018. [3](#)
- [38] Tao Zhou, Linyuan Lü, and Yi-Cheng Zhang. Predicting missing links via local information. *The European Physical Journal B*, 71(4):623–630, 2009. [3](#)
- [39] Chunhui Zhu, Fang Wen, and Jian Sun. A rank-order distance based clustering algorithm for face tagging. In *CVPR 2011*, pages 481–488. IEEE, 2011. [2](#)